

Fermilab

\bar{p} Note #421

THE FERMILAB $\bar{p}p$ COLLIDER: MACHINE AND DETECTORS

E. Malamud

THE FERMILAB $\bar{p}p$ COLLIDER: Machine and Detectors

Ernest Malamud

Invited talk presented at the
Fifth Topical Conference on
Proton-Antiproton Collisions
St. Vincent, Italy, February 26, 1985

I. INTRODUCTION

This paper is a condensed version of the talk presented at the conference. The principle objective of the talk was to inform the community of the present status of the collider at Fermilab. Since progress is rapid on both the accelerator and the detectors, much of the material presented would be out of date by the time these proceedings are published. Many photographs were shown of the current state of construction. These will not be reproduced here.

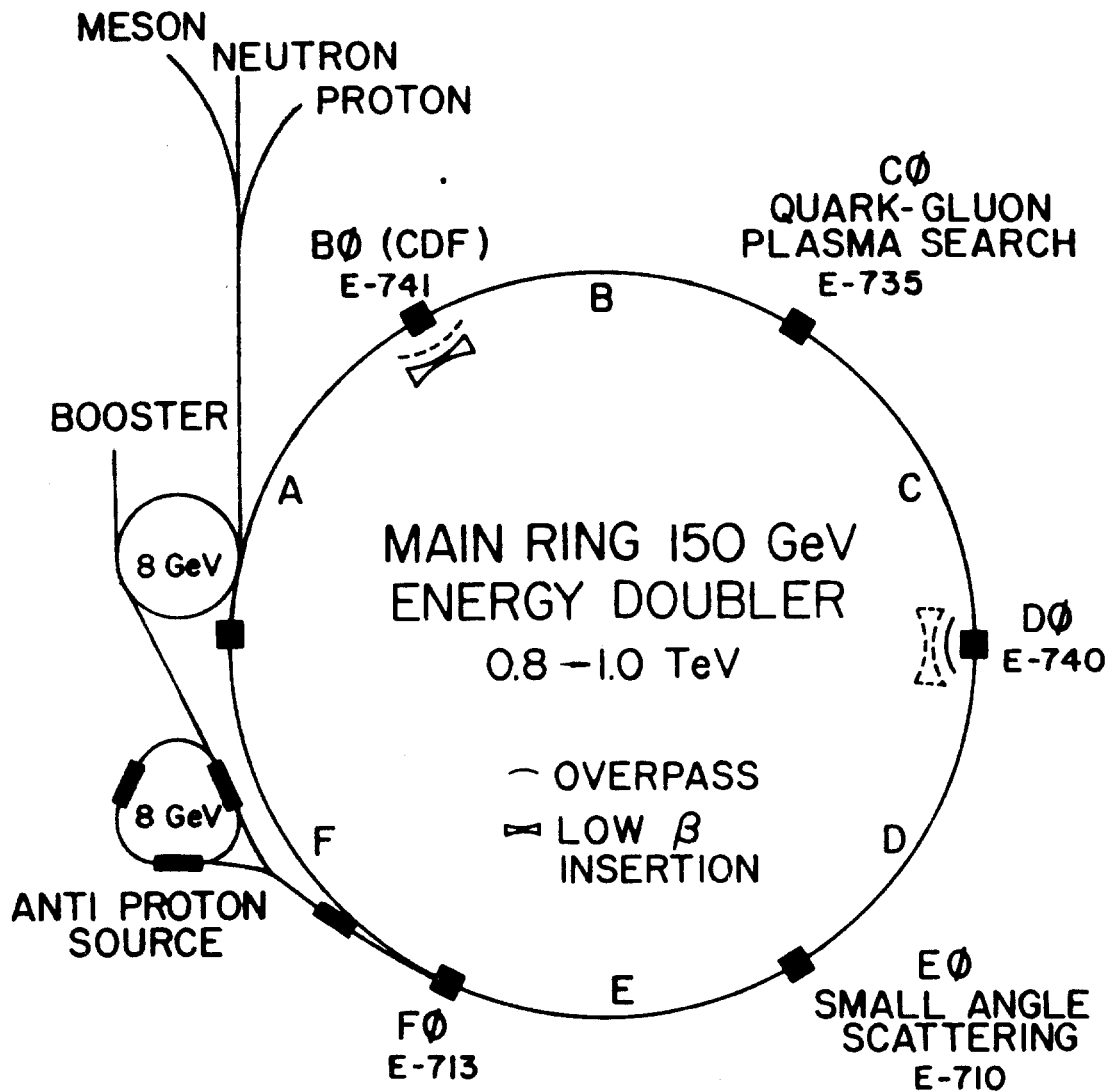


Figure 1

Most of the major parameters of both Fermilab Collider and the two major detectors were given last year at the Berne workshop in the session on the Fermilab program in talks by M. Harrison, D. Theriot, and M. Marx.¹⁾ More details can be found in the design reports.²⁾

Figure 1 shows the Fermilab geography. The 4 major components of the antiproton source are the Main Ring (MR), the Target Station, the Debuncher, and Accumulator. These elements are used to produce antiprotons and compress them in phase space for injection into the MR and subsequently into the Energy Doubler (ED).

There are 5 approved collider experiments:

1. E-735. C0. Search for a Deconfined Quark-Gluon Phase of Hadronic Matter. Collaboration of Duke University, Iowa State University, Fermilab, University of Notre Dame, Purdue University, and the University of Wisconsin.
2. E-710. E0. Measurements of Elastic Scattering and Total Cross Sections. Collaboration of the University of Bologna, Italy and five U.S. institutions: Cornell University, Fermilab, Northwestern University, University of Maryland, and George Mason University.
3. E-741. B0. (Collider Detector at Fermilab -- CDF). Large multi-purpose detector being built by an international collaboration of Italy, Japan, and the United States. Following is the list of institutions: Argonne National Laboratory, Brandeis University, University of Chicago, Fermi National Accelerator Laboratory, INFN--Frascati, Italy, Fukui University, Japan, Harvard University, University of Illinois, KEK, Japan, Lawrence Berkeley Laboratory, University of Pennsylvania, INFN-University of Pisa, Italy, Purdue University, Rockefeller University, Rutgers University, Saga University, Japan, Texas A&M University, ICRR, Tokyo University, Japan, Tsukuba University, Japan, and University of Wisconsin.
4. E-740. D0. Large multi-purpose detector to be built by the following collaboration: Brookhaven National Laboratory, Brown University, Columbia University, Fermilab, Florida State University, Lawrence Berkeley Laboratory, University of Maryland, Michigan State University, Northwestern University, University of Pennsylvania, University of Rochester, CEN Saclay, France, State University of New York (Stony Brook), and Virginia Polytechnic Institute.
5. E-713. F0. University of California, Berkeley. Search for Highly Ionizing Particles using Lexan plates.

I will describe E-735 and E-710 briefly and present more detail on the large detectors at B0 and D0.

II. OVERPASSES and LOW BETA INSERTIONS

Overpasses.

In the same tunnel are the "old" MR operating at 150 GeV, and the 1 TeV ED currently operating at 0.8 TeV. Having two rings in one tunnel is a complication for the two major detectors.

The normal vertical separation of the planes of the MR and ED is 0.65 meters. At D0 the MR has been displaced upwards (and slightly inwards) for a MR - ED separation of 2 meters, making the MR the first non-planar large synchrotron. This overpass works successfully at MR intensities of over 10^{13} (10^{10} /bunch). Future accelerator studies will measure the performance of the MR with single intense bunches (10^{11}). The overpass will pass through the future D0 detector near the outside of the central calorimeter (leakage section) as seen in figure 12.

The 6 m overpass at B0 requires major civil construction to be done during the long shutdown starting in the fall of this year. It will completely bypass the B0 detector as can be seen in figure 11.

Storage Studies.

The performance of the ED as an 800 GeV storage ring is being investigated in regularly scheduled study periods. Proton beams have been stored for hours on several occasions and the inferred lifetime is greater than 24 hours. Measurements of transverse profiles are made with a flying wire. The transverse stability is excellent although some growth in transverse emittance is observed. Future studies will investigate this as well as the longitudinal stability of intense single bunches. Stores are sometimes terminated by hardware failure. The stores provide valuable data on machine reliability for investigation of each problem in detail and implementation of a solution.

Low Beta Insertions.

Once the beam is stored, the low beta insertion installed at B0 can be turned on and the beam "squeezed". To reduce β^* from the normal straight section value of around 100 to 1 meter in each plane, and achieve the design luminosity of 10^{30} cm^{-2} sec^{-1} , four additional quad circuits are energized. The quadrupoles in these circuits are similar to those of the ED but with a superconducting cable capable of carrying currents up to 6000 amps. There are 30 steps in the current program to adiabatically change the ED lattice from the fixed target to the low beta configuration. The total time for the "squeeze" is less than 2 minutes.

Using Schottky pickups the tunes are measured (to accuracy of 2×10^{-5}) and corrected through all 30 steps of the squeeze. Measurements of the uncorrected closed orbit during the squeeze show distortion maxima of ± 5 mm vertically and ± 2 mm horizontally. The high field quadrupoles are cantilevered to insert into the detector. The precision of the ED beam measurements has confirmed their mechanical stability.

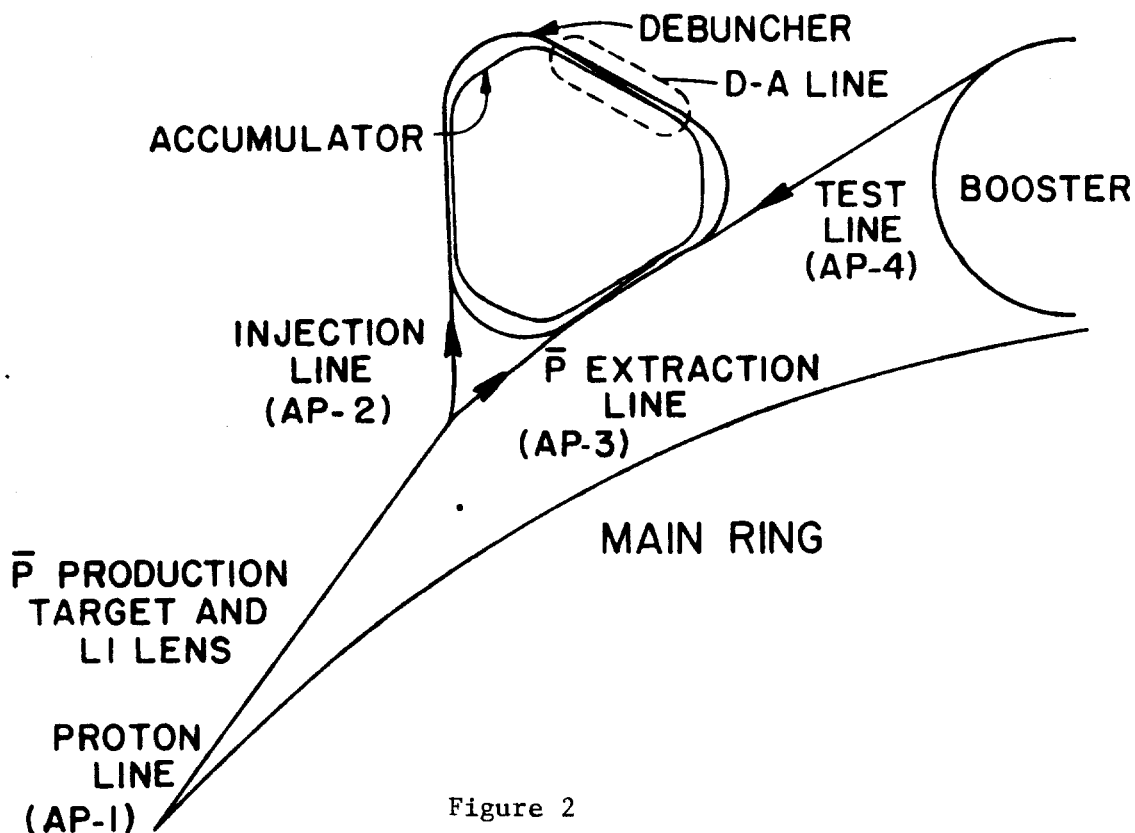


Figure 2

III. THE ANTIPROTON SOURCE

Overview.

The source is the ensemble of beam lines and rings shown in figure 2. The antiproton source is based on the stochastic cooling method of S. Van der Meer and his colleagues³⁾ and is designed to accumulate 4×10^{10} antiprotons in 4 hours. 1.8×10^{11} are removed from the high density core and divided equally among 3 antiproton bunches. Subsequent accumulation cycles should be shorter.

Early Commissioning

Commissioning is done parasitically while the fixed target program or storage/squeeze studies are in progress as illustrated by the time line in figure 3.

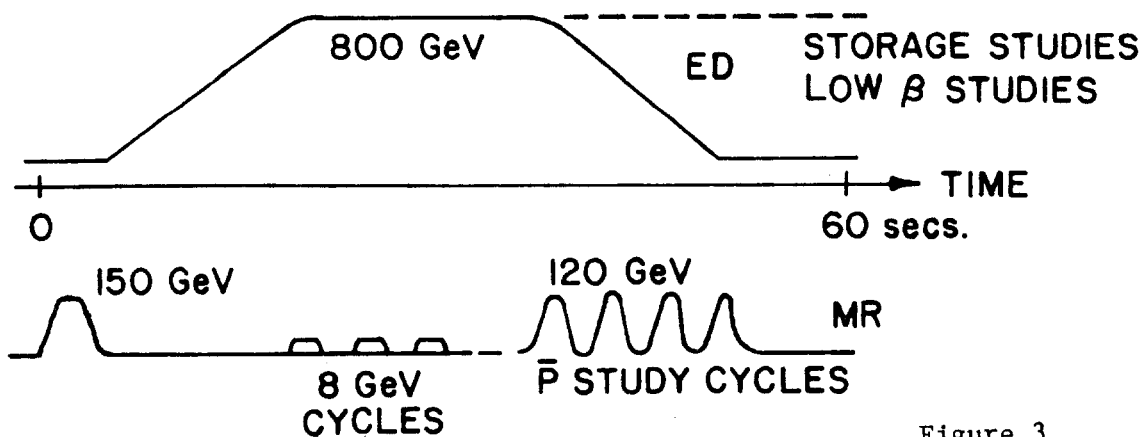


Figure 3

Commissioning steps that have been accomplished (all in 1985):

- Jan. 26. Beam extracted at 120 GeV from the MR and transported in AP-1 to the target station.
- Feb. 11. Beam extracted at 8 GeV and transported in AP-1 to the Target Station.
- Mar. 16-17. 120 GeV bunch rotated beam extracted and focussed to a 1.1 mm spot at the target location.
- Mar. 24. 8 GeV beam focussed to 4.2 mm spot.
- Mar. 29-Apr. 1. 8 GeV beam transported in AP-1 and AP-2 to the Debuncher.
- Apr. 5-6. First attempts at injection into the Debuncher.

A series of commissioning steps are planned for the spring and summer of this year (refer to figure 2):

1. Debuncher commissioning using 8 GeV protons. Correct direction, wrong polarity.
2. Extraction line (AP-3) and Accumulator commissioning using 8 GeV protons. Wrong direction, correct polarity.
3. Insertion of target and lithium lens.⁴⁾ Yield measurements and tuneup of the Debuncher on \bar{p} 's.
4. Commissioning of the D/A line (Debuncher-Accumulator transfer) using either protons from the Debuncher (wrong polarity, correct direction), or protons from the Accumulator (correct polarity, wrong direction).
5. Tuneup of the stochastic cooling systems in both rings using protons. Correct direction, wrong polarity.

6. Stacking, and cooling studies in both rings with \bar{p} 's.
7. Extraction of \bar{p} 's, transfer to the MR, acceleration, coalescing, and transfer to the ED.

During the long shutdown scheduled to start in the fall of 1985 for the construction of the B0 overpass, and the D0 experimental area, antiproton source studies can continue with the Booster. A second extraction point from the Booster and a target station for reducing the Booster intensity by using diffractively scattered 8 GeV protons has been constructed. This beam (AP-4) can be injected into the Debuncher and Accumulator rings. (wrong polarity, correct direction).

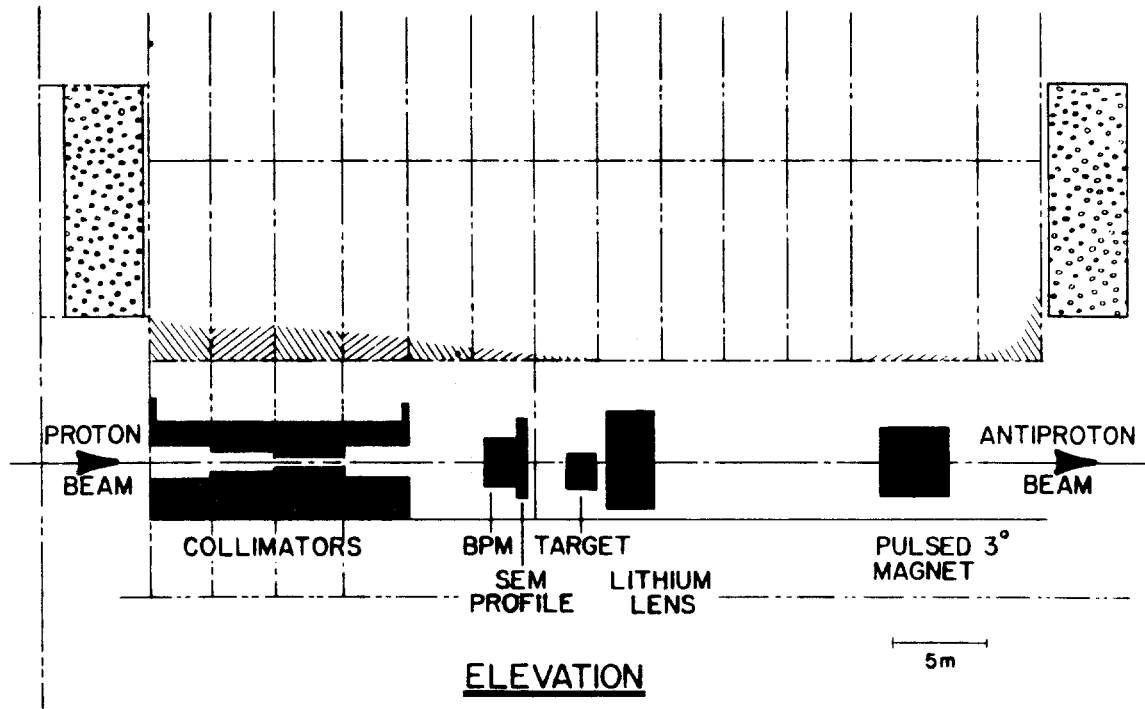


Figure 4

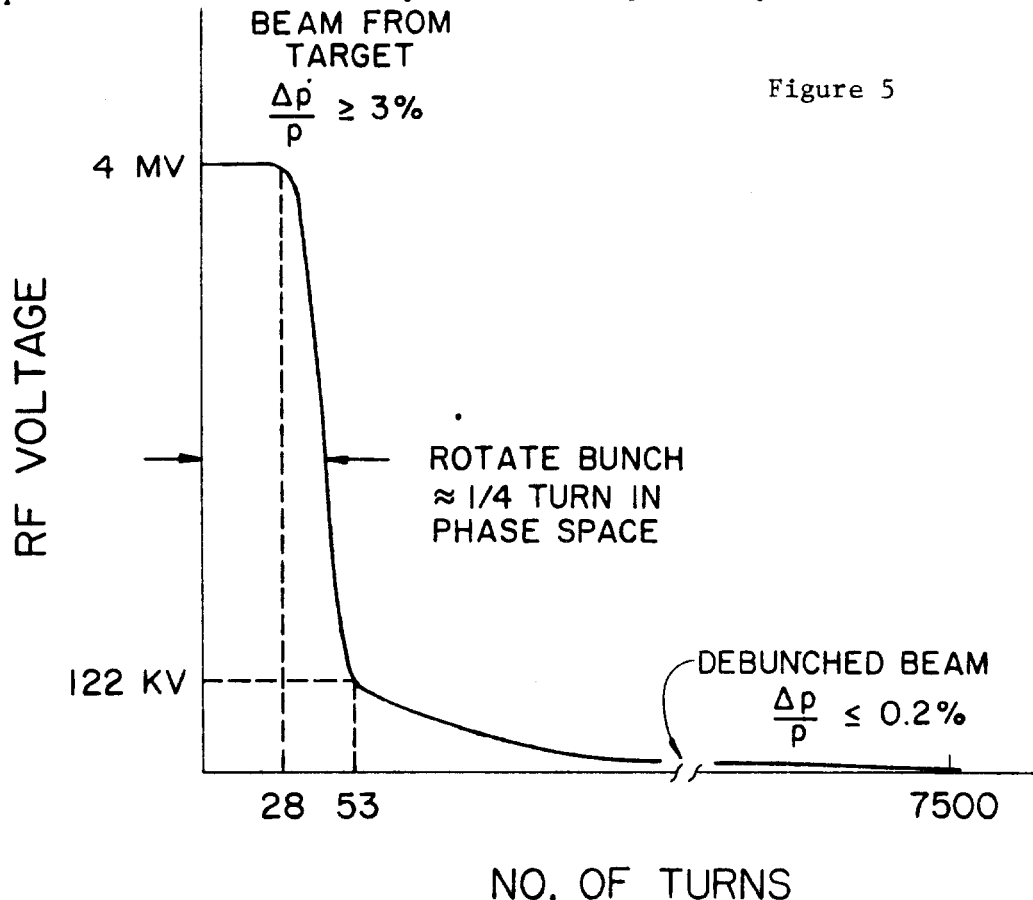
The Target Station.

Shown in figure 4 is an elevation view of the target station. Each of the 13 removable steel modules serves both as a radiation shield and a stable mounting for target components.

Stochastic cooling is more effective if the initial beam size and time spread are minimized. Beam size is limited by heating in the 6 cm long tungsten-rhenium target. The time spread is reduced to less than one nsec. by first adiabatically lowering the MR RF voltage until the bunch has a momentum spread of 0.03%. The RF voltage is then suddenly snapped on to 4 MV and the entire bunch rotates until the time spread is minimized and the momentum spread is 0.4%.

Antiprotons are collected in a 60 mrad cone using a pulsed lithium lens with the following parameters: peak current 620 kA with a half sine wave of 340 microsec., gradient=1000 T/m. The most recent lens was run at 620 kA for 90,000 pulses and then failed. Failure was in a weld joint in the water septum. Pressures of up to 2000 psi in the water develop at the full peak current. Lens 5 and 6 now under construction will have a different design to avoid this problem.

An earlier lens has been used at CERN to focus the incident proton beam. It ran at 300 kA peak and was used successfully for 1.6×10^6 pulses at a beam intensity of 1.3×10^{13} protons/pulse.



The Debuncher.

The purpose of the Debuncher is to reduce the large momentum spread of the 8 GeV antiproton beam by RF bunch rotation and adiabatic debunching. This is the opposite of the process in the MR described above and is illustrated by figure 5. Debunching is done by 6 RF cavities each developing 750 KV. Originally the design called for 8. The space freed up is used for a diagnostic cavity for exploring the aperture.

The circumference of the Debuncher is 200 nsec. longer than the Accumulator. This gap is needed for extraction from the Debuncher and is maintained by a special $h=4$ gap preserving RF system illustrated in figure 6. The bucket height in this RF system is greater than the beam energy spread so it creates a barrier.

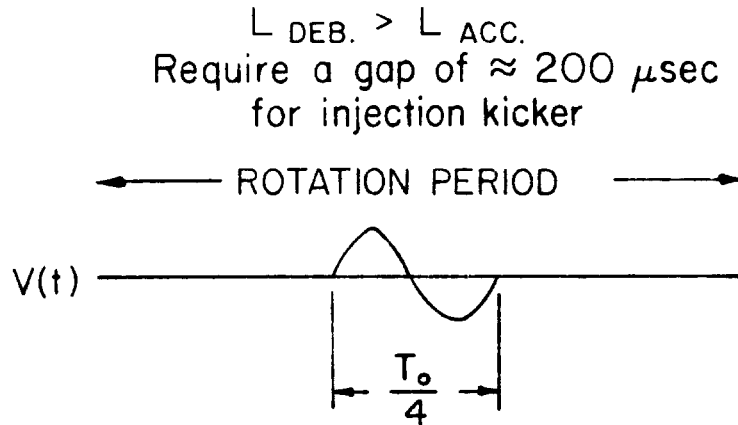


Figure 6

The reduction in momentum spread from 3% by a factor of 15, takes only 10 msec. so the remaining time between MR cycles can be used for betatron stochastic cooling in the Debuncher. This is designed to reduce the beam emittance in each plane from 20π to 7π mm-mrad, an emittance that can be reliably transferred into the 10π acceptance of the Accumulator ring with negligible beam loss. In addition to cooling the beam to fit into the Accumulator it is desirable to make the beam small horizontally since stacking in the Accumulator is done in part by a pickup that senses a particle's momentum from its position in a high dispersion straight section. Betatron oscillations add undesirable noise to the stacking process. In the Debuncher horizontal and vertical pickups sense the positions in a zero-dispersion region. The signal is amplified and applied to a kicker 13 quarter wavelengths in betatron phase away. To optimize the signal-to-noise ratio the pickups and preamplifiers are cooled to 77°K .

The Debuncher was completed, under vacuum, power tested, and ready for initial beam studies on April 4.

The Accumulator.

The function of the Accumulator is illustrated in figure 7. The Accumulator is designed to accept up to $8 \times 10^7 \bar{p}'\text{s}$ from the Debuncher as often as every two seconds with the following phase space parameters: $\epsilon_V = \epsilon_H = 10\pi$, $\Delta p/p = 0.2\%$. In the Accumulator the $\bar{p}'\text{s}$ are stacked in momentum space and compressed into a high density core with the following properties: $4 \times 10^{11} \bar{p}'\text{s}$, $\epsilon_V = \epsilon_H = 2\pi$, $\Delta p/p = 0.05\%$.

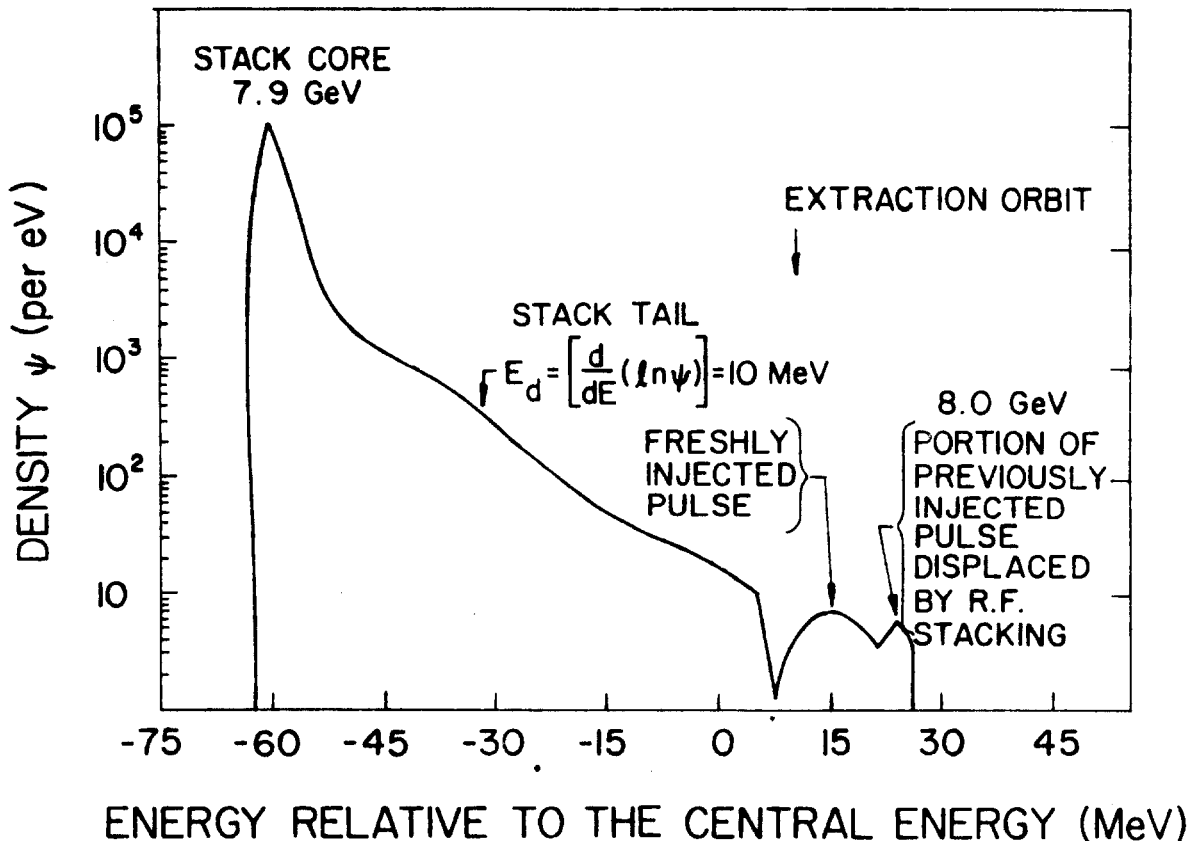


Figure 7

The Accumulator lattice has 3 high dispersion and 3 zero dispersion straight sections. Figure 8 shows the layout of the six independent stochastic cooling systems which provide horizontal and vertical betatron, and momentum cooling for both the newly injected batch of antiprotons (the stack tail) and the circulating beam (the core). The momentum cooling systems use pick-ups in high dispersion regions and kickers in zero dispersion ones. The core betatron cooling goes from zero dispersion to zero dispersion, and the stack tail betatron cooling from high dispersion to high dispersion.

As in the Debuncher, Accumulator stochastic cooling pickups are cooled to 77° K. A superconducting notch filter reduces microwave power at frequencies corresponding to particles in the core, and assists in shaping the gain vs. momentum curve in the stack-tail system.

The Accumulator has a bakeout system designed for 300° C. The last magnet was installed in the Accumulator on April 8, 1985 and alignment and vacuum welding is rapidly nearing completion.

ACCUMULATOR			
STOCHASTIC COOLING SYSTEMS			
---	Stack Tail MOM	1-2 GHz	150 db uses superconducting notch filters
----	Stack Tail Betatron	1-2 GHz	125 db
-----	Core MOM	2-4 GHz	110 db
-----	Core Betatron	2-4 GHz	106 db

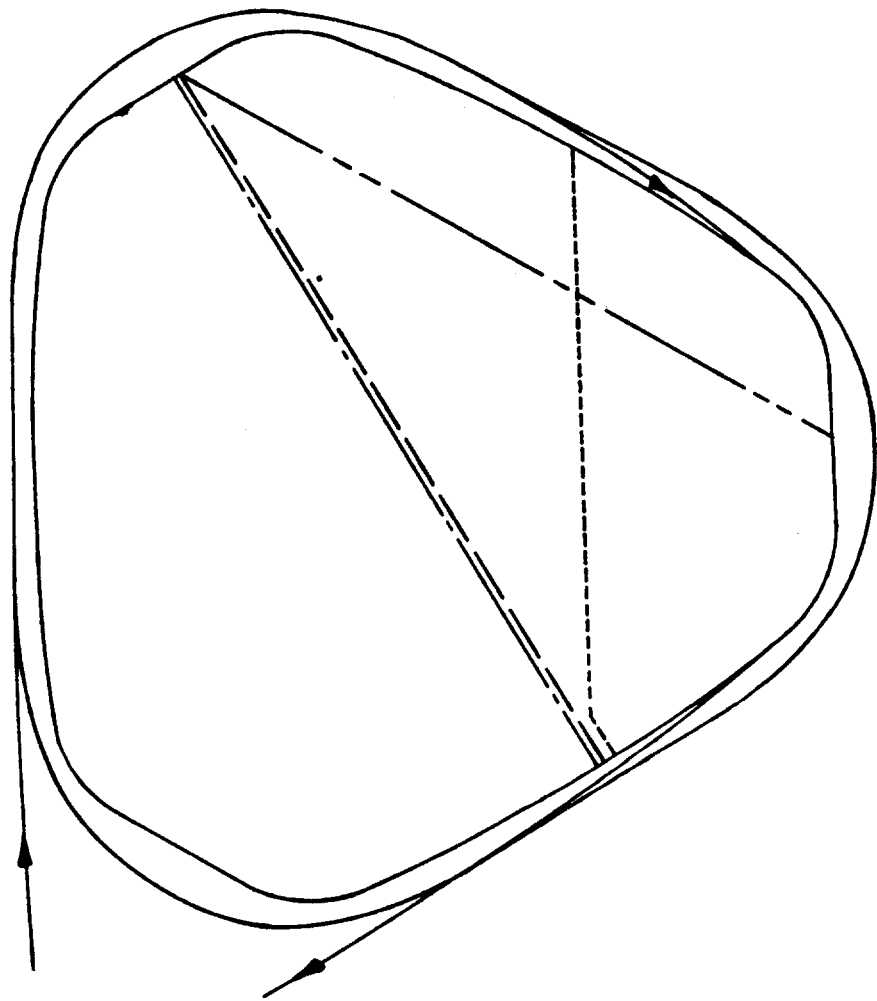


Figure 8

Beam Diagnostics.

Commissioning of the beam lines and rings is made easier by good diagnostics and a flexible computer control system. The beams are instrumented with Secondary Emission Monitor crossed x- y- grids consisting of 10 micron titanium strips with either 1.5 or 3.0 mm grid spacing. The electronics are a modification of the microprocessor based SWIC scanners used in the experimental area beam lines at Fermilab. The least count sensitivity is 5×10^{-15} Coulomb. Additional beam line diagnostics are loss monitors, current monitors, gap detectors, and, in AP-2 a Cerenkov counter for \bar{p} yield measurements.

Each quadrupole in the ring has either a vertical or horizontal electrostatic beam position monitor. The total is 120 in the Debuncher and 90 in the Accumulator. These monitors have single turn capability for 10^9 particles and multiturn capability for 10^7 particles. In addition are current monitors, Schottky pickups, and a gas ionization profile monitor.

The computer system used is an extension of the successful ACNET system.⁵⁾ A front-end PDP-11/44 is dedicated to the antiproton source control requirements. This in turn communicates via a serial link to 14 nodes each of which has several CAMAC crates containing a mixture of "dumb" and smart (microprocessor) modules. There are approximately 100 distributed microprocessors in the antiproton source control system. The front-end computer communicates via a VAX system with the console computers. There are presently 16 consoles in ACNET. In practice 3 of these consoles are used for commissioning of the antiproton source. However, any console can control any part of the accelerator. This allows the very useful ability to correlate \bar{p} source variables with e.g. variables in the MR.

Operating Scenarios.

The transfer process starts by adiabatically capturing antiprotons from the core using a single $h = 2$ bucket and slowly moving the beam to the extraction orbit. This bunch has a longitudinal phase space of 1.5 eV-sec and is too large to accelerate in the MR. Therefore it is bunched at the MR frequency, 52.8 MHz, in the Accumulator and then extracted in a single turn using a shuttered kicker.

In the MR 13 bunches are accelerated to 150 GeV and then coalesced into a single bunch and rotated prior to injection into the ED. The whole cycle is repeated until 3 bunches of antiprotons are circulating along with three bunches of protons that have been injected earlier.

IV. SMALLER EXPERIMENTS

E-735, a search for a deconfined quark gluon phase of hadronic matter, shares the C0 straight section with the proton and antiproton

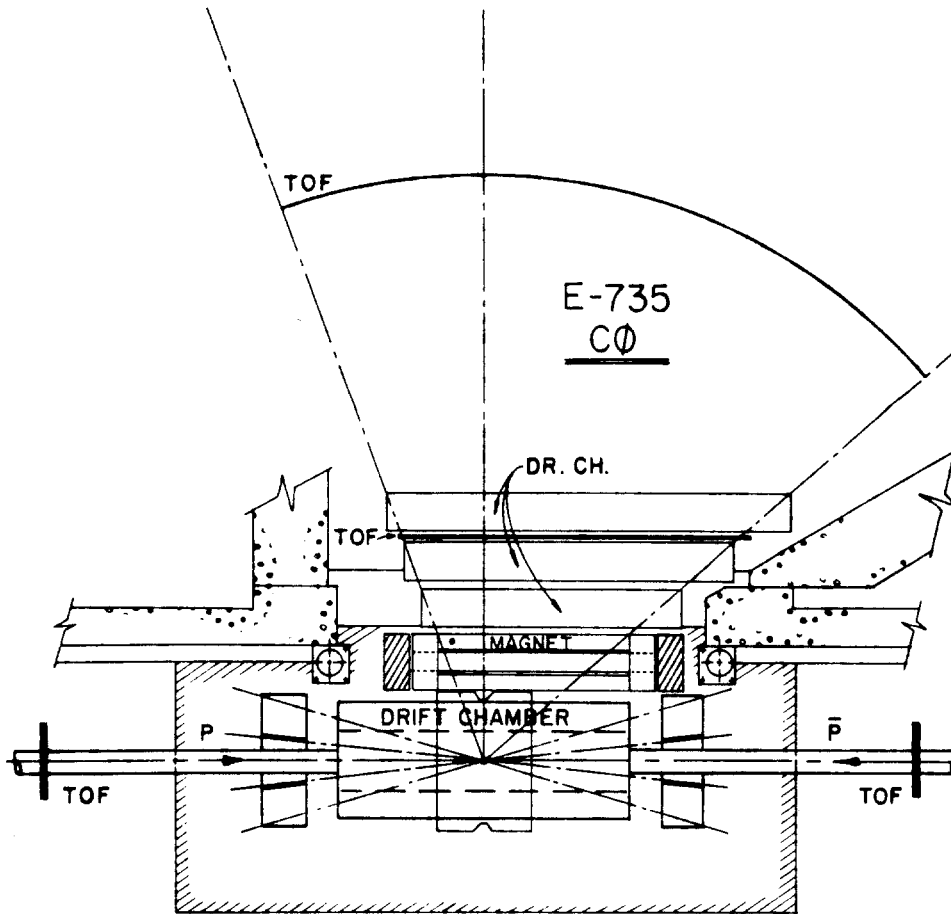


Figure 9

beam abort systems. A plan view is shown in figure 9. There are several signals that could indicate a transition from a hadron "gas" to a quark-gluon "gas". The correlation between average $\langle p_t \rangle$ (temperature) and dn_{\pm}/dy (at $y=0$) (entropy density) will be studied by a drift chamber system covering most of the solid angle and a magnetic spectrometer covering a limited region in phase space ($-1.0 \leq y \leq 0.4$, $\Delta\phi = 25^\circ$). The design luminosity at C0 is 1.3×10^{28} (no low beta insertion). At this luminosity and at total charged multiplicities of >100 , >150 , >200 , E-735 will be able to record event rates/day of 7×10^5 , 2×10^4 , and 500 respectively. The experiment should be able to reach densities in the central region dn_{\pm}/dy (at $y=0$) of 25 to 30. Enhanced strange particle production is another possible signal of a phase change. Time of flight counters can achieve $\pi/K/p$

separation over the range (0.3 p 1.4) GeV/c. A future phase of the experiment will use a scintillating glass hodoscope to look for enhanced direct photon production.

E-710 shares E0 with the MR to ED transfer lines (both directions). This experiment can measure d/dt over a momentum transfer range from the Coulomb region out to -0.11 (GeV/c) at $\sqrt{s} = 300$ and -4.8 (GeV/c)² at $\sqrt{s} = 2000$. A 4π scintillation counter detector will be used to obtain σ_T . In order to measure into the Coulomb region at these high energies detectors are placed deep into the accelerator lattice as seen in figure 10.

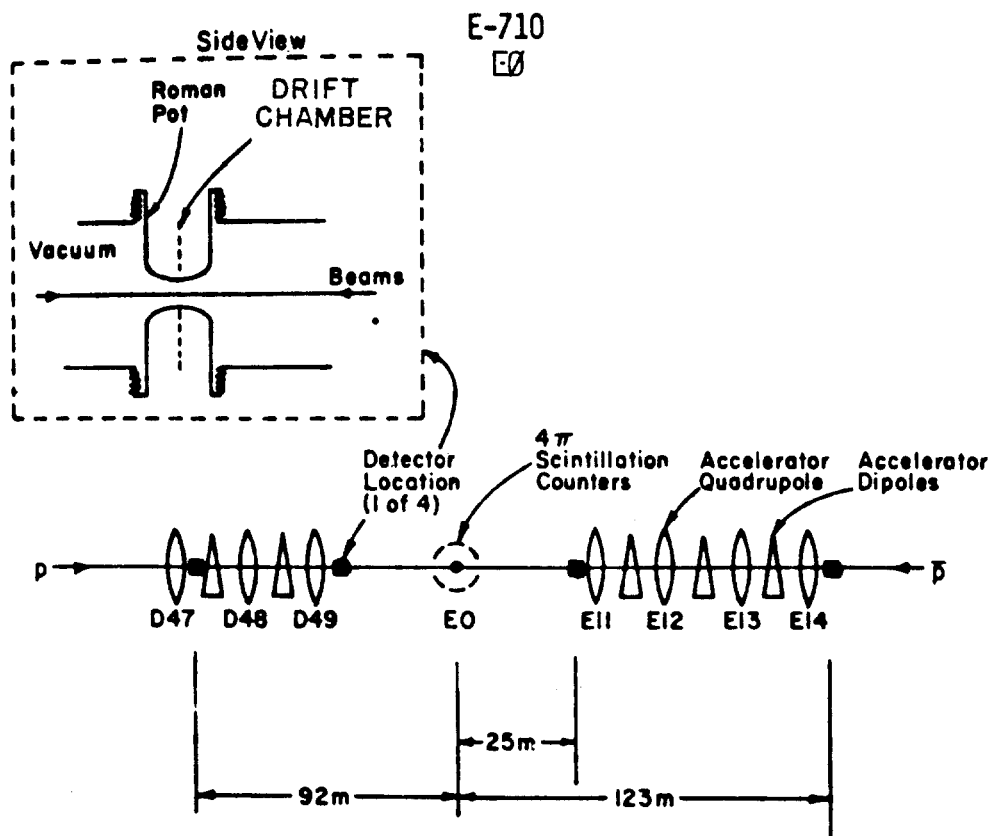


Figure 10

The final part of my talk concerns the major detectors at B0 (E741, CDF) and D0(E740).

V. THE COLLIDER DETECTOR AT FERMILAB

This powerful detector is being constructed by an international collaboration between Italy, Japan, and the United States. All three countries are participating heavily. An elevation view of the B0 detector is shown in figure 11. Particles produced between 2° and 10° pass out of the central detector through a hole in the end plug calorimeter and enter the forward and backward detectors.

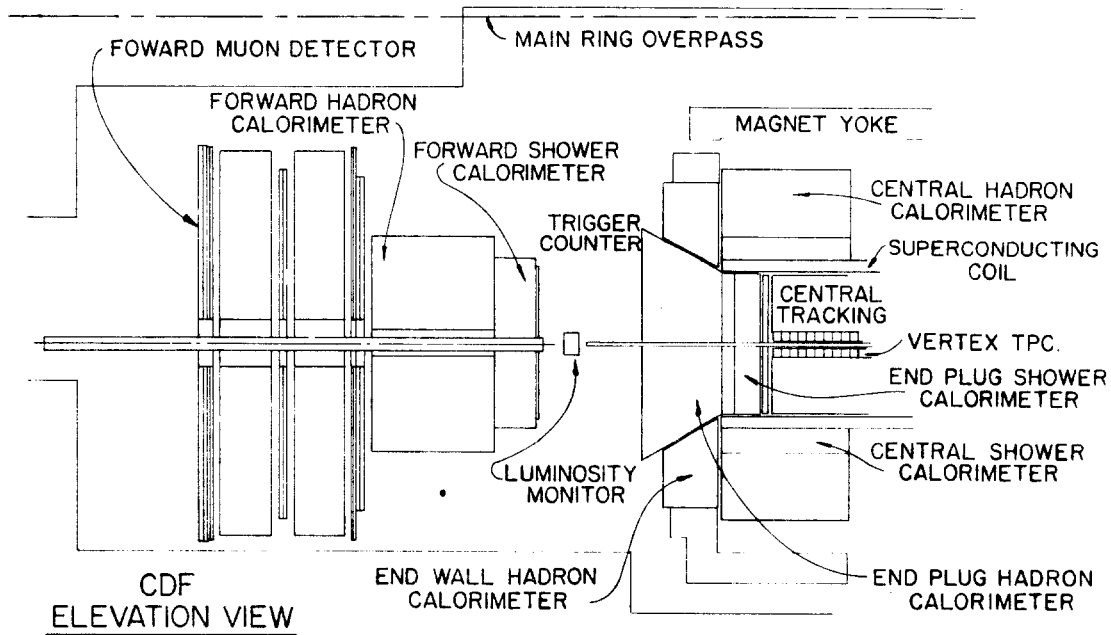


Figure 11

The central part of the detector is rapidly nearing completion and could be ready to roll into the collision hall for an initial test this summer. Since the overpass will not exist at that time this early test would have to omit the central tracking chamber (CTC) since the MR beam pipe presently goes through that region.

In the talk at this conference a series of photographs of various components of the central detector were shown.

1. The superconducting solenoid built in Japan is 3 meters in diameter and 5 meters long. The conductor is cooled and supported by means of an external cylinder of aluminum. The thickness of the coil and its cryostat is approximately 1 radiation length (RL) and 0.5 absorption length (AL). On March 24 the superconducting solenoid was successfully tested in the magnet yoke at its design field of 1.5 T.

2. Surrounding the magnet are the shower counters and hadron calorimeters. The shower counters in the region between 90° and 33° are made of a lead scintillator sandwich read out with waveshifter bars and light pipes. A strip proportional chamber at a depth of 5 RL provides fine grained information on the shower location and helps electron/photon separation. Outside the hadron calorimeter are the central muon detectors composed of four layers of drift chambers instrumented with current division. The instrumentation for the hadron calorimetry comes from Italy.
3. Between 33° and 10° the shower counters are lead alternating with gas filled proportional counters fabricated out of resistive plastic tubes with cathode pad readout. A strip proportional chamber is also provided in these detectors at the shower maximum to provide information about shower location. Outside the shower counters are located the hadron calorimeters.
4. Between 30° and 10° the hadron calorimeters are steel and proportional pad chambers.
5. Tracking is accomplished by means of the CTC and the Vertex Time Projection Chamber (VTPC). The CTC in conjunction with the 1.5 T solenoidal field allows for precision measurement of individual charged particles with p_t less than 40 GeV/c. The CTC is built with 9 supercells of drift chamber. Five superlayers have axial wires and four interleaved small angle stereo layers are skew at an angle of 3° with respect to the axis.
6. The VTPC fits inside the CTC and consists of 8 cells along the beam. Each cell has the HV plane in the middle and the drift is towards the two ends.
7. Inside the VTPC is a 5 cm. diameter 2 mm thick beryllium beam pipe. The beam at the collision point has a size of about 60 microns. With such a small transverse size a very high resolution vertex detector will be useful for identifying long lived particles. For this reason a silicon strip detector that fits inside the VTPC is being developed by the Pisa group. That group has also made important design contributions to the CDF electronics.

A more complete description of the detector can be found in the recent paper by Tollestrup.⁶⁾

The detector is being rapidly assembled. The central detector calorimetry is nearly complete and is being calibrated in test beams. The tracking chambers are being manufactured, and the VTPC will be ready for preliminary beam tests in the fall of 1985. The spring of 1986 will see all components ready for test with the beam in preparation for the first physics run in the fall of that year.

VI. The D0 DETECTOR

Introduction

The D0 detector will:

- Increase the total number of collisions observed (doubles the return on the Fermilab Collider investment)
- Provide a different focus from CDF, UA1, and UA2 on short distance physics.

We have learned a great deal from CERN and are learning more at this conference. Most important for the design of the D0 detector is the observation that at high p_t everything is "jetlike" and jets are "clean". This is illustrated by comparing the track and calorimeter information for events in UA1 and UA2. The design criteria and goals for the D0 detector are based on a well known physics menu and the experience at CERN. We have the advantage of being able to capitalize on that experience, but the disadvantage of coming on later.

There is no central magnetic field. We gain in simplicity in straight line tracking, compactness, which permits full calorimetric coverage, very little material in front of the calorimeter, and symmetric measurement of charged and neutral particle energies.

Jets are identified cleanly and directly by a high resolution, fine grained calorimeter. At these energies the best instrument is a calorimeter where $\Delta E/E \propto 1/\sqrt{E}$ rather than a spectrometer ($\Delta p/p \propto p$).

Neutrino detection is accomplished by good resolution in missing p_t . This is done by minimizing dead regions, having fine grained calorimetry to provide good angle measurements, and hermetically covering the region down to 1° from the beam. The D0 calorimetry has a high degree of segmentation, both in transverse tower size and longitudinally. The transverse segmentation will permit better electron discrimination by improved rejection of charged hadron-electron overlaps, and improved detection of electrons near jets. The longitudinal segmentation permits measurement of shower profiles for electron hadron discrimination.

For muons, magnetized iron gives the sign, and large total thickness permits identification even in the core of jets. The iron plus calorimeter total 13.3 AL at 90° and 18 AL at 11° , the minimum angle for muon coverage. The maximum detectable momentum (3σ) will be about 300 GeV/c and the multiple scattering limited momentum resolution is 20%. Tests of hadron punchthrough have confirmed the choice of parameters.

For electrons excellent energy resolution is stressed. The highly segmented calorimeter coupled with a transition radiation detector (TRD) provides excellent e/π separation.

The three main parts of the detector shown in figure 12 are a central tracking system, the liquid argon uranium calorimeters, and the muon detector.

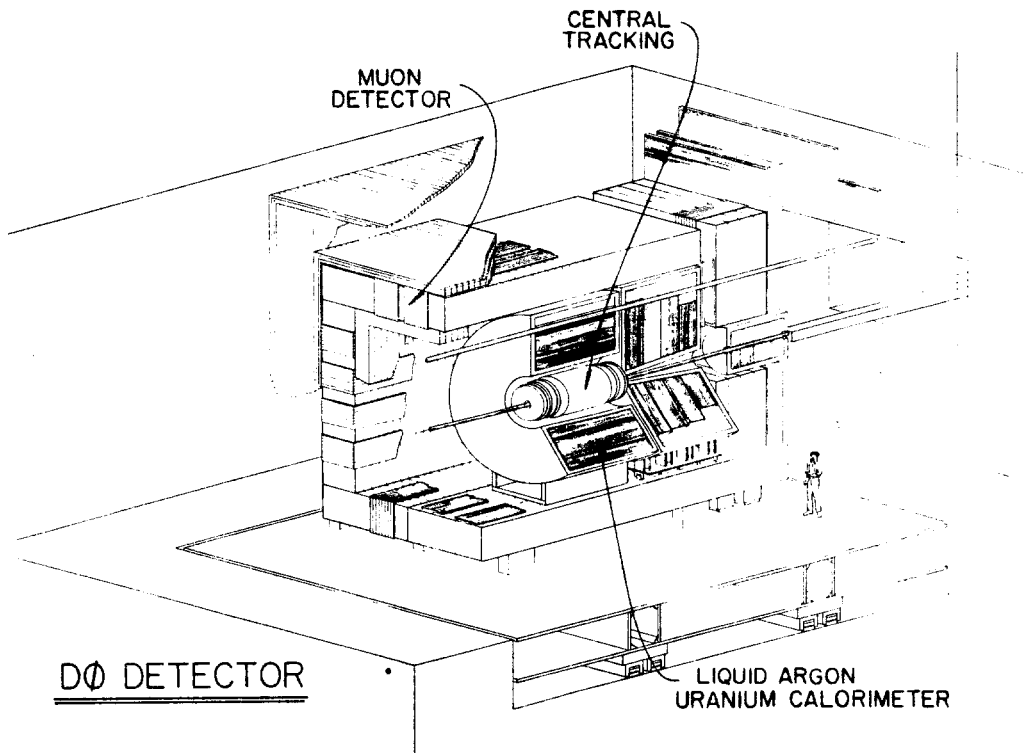


Figure 12

The Central Detector

The central detector consists of drift chambers and TRD's surrounding a microvertex detector. The purpose of the microvertex detector is to identify charged particles before the TRD, and observe separated decay vertices with a design goal of ~ 100 micron spatial resolution.

The detailed design of the central detector has evolved from the design report²⁾. Some of those changes will be described:

The TRD sections will probably be alternated with drift chamber sections and studies are underway to investigate the feasibility of combining the X-ray and charged track coordinate measurements. The TRD's originally were to have been two sections, each composed of a stack of lithium foils. More recent designs use 3 sections made of polypropylene foils.

The central and forward drift chambers measure charged track angles and dE/dx . The forward/backward chambers will use r, ϕ segmentation to better handle the expected high multiplicities. 24 samples of dE/dx provide 20:1 rejection against e^+e^- pairs. The system

has sufficiently good two-track resolution to permit identification of electrons in or near jets. The tracks in the drift chambers will provide a vertex for use in the muon trigger.

The Liquid Argon - Uranium Calorimeter

This is the heart of the detector and essential to the physics objectives. It is also the most costly part thus strongly influencing the schedule. The calorimeter has been divided into 5 portions: a central calorimeter, two end cap calorimeters, and two plug calorimeters. The exact form of the plug calorimeters is still under discussion within the collaboration and may be changed to gas calorimetry. Accurate angle measurements are important for forward/backward particles whereas energy resolution is less important in determining missing p_t .

Uranium was chosen for (1) high density which leads to a compact detector and thus reduces the cost of the outer (muon) detector, (2) excellent energy resolution (electrons - $0.12/\sqrt{E}$, hadrons - $0.4/\sqrt{E}$), and (3) electromagnetic response equal to hadronic response. However, the last point, compensation, needs to be confirmed by further tests which are now being prepared. Liquid argon was chosen as the shower readout medium for the following reasons: (1) only a few mm thickness is needed to obtain a good signal, thus also contributing to detector compactness, (2) stability of a unit gain ion chamber, (3) simplicity of calibration using charge injection, (4) easy to make projective towers and have good transverse and longitudinal segmentation, and (5) no radiation damage. The calorimeter is designed so no detector cracks or dead spaces point to the interaction region. Because of unit gain and stable response of this system, we expect to be able to control systematic effects at the 1/2% level.

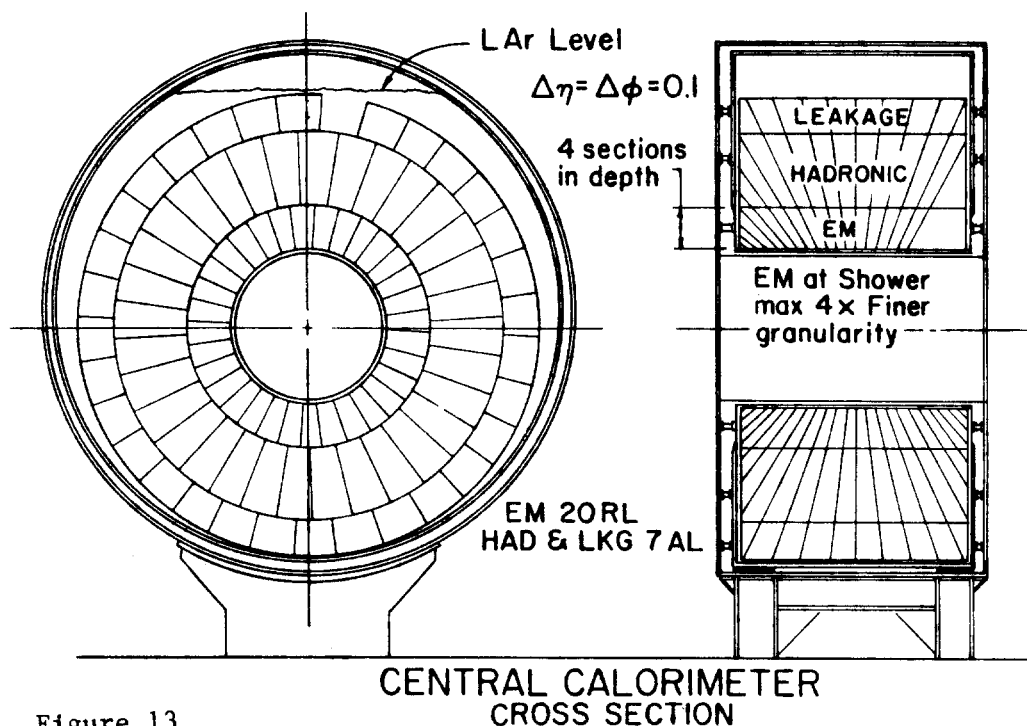


Figure 13

Figure 13 shows elevation views of the central calorimeter. The central calorimeter consists of 16 azimuthal wedges, 165 cm. thick, with three longitudinal sections. It is presently planned that the electromagnetic (EM) and hadronic (HAD) sections would be constructed of pure uranium, whereas the leakage section would use copper plates. The front EM compartment has 0.5 RL absorber plates and is read out four times longitudinally to enable us to reject non-electromagnetic backgrounds. The size of the transverse towers is approximately 6x6 cm with 1 cm strips located at the peak of the shower. The HAD section has three longitudinal readouts with 4 mm thick uranium plates and one leakage section with very coarse sampling. The typical hadronic tower is 15x15 cm².

END CAP CALORIMETER

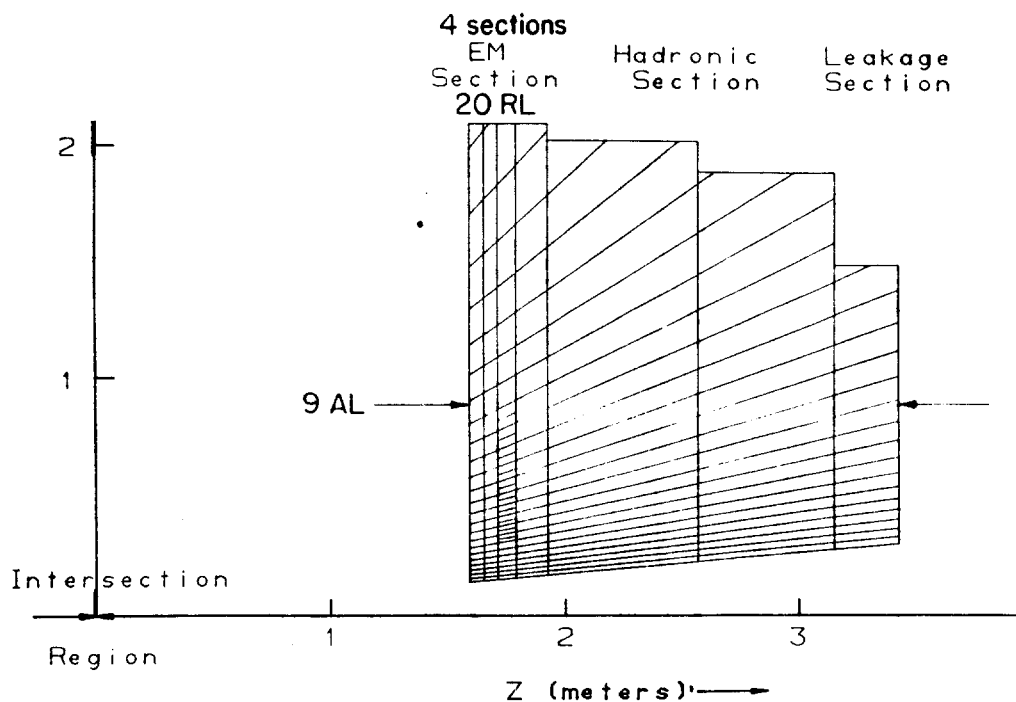


Figure 14

An elevation view of the end cap calorimeter is shown in figure 14 to illustrate its segmentation. The end cap calorimeters cover the region down to 5. They have the mechanical simplification of having all the absorber plates standing vertically, and the complication of having readout towers which vary greatly in size, with very high readout density close to the beam. The end cap calorimeters will use alternating uranium and copper plates.

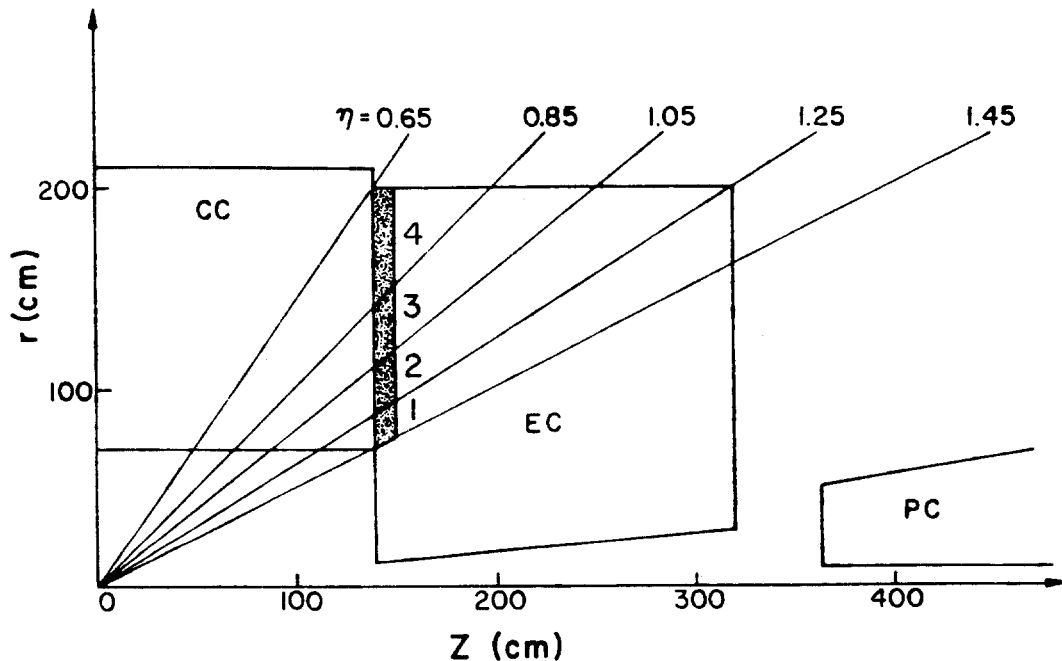


Figure 15

Monte Carlo studies using a particular model for jet production have been made to evaluate the relative importance of various contributions to the resolution in missing p_t . Referring to figure 15 it was found that the resolution was relatively insensitive to the size of the beam hole but that the main contribution came from the 10 cm. thick dead layer between the central and end cap calorimeters. Region 1 -- near 45 is especially important. From this study evolved the nesting concept for the central and end-cap calorimeters shown in figure 16. This effectively eliminates the problem and also, the cryostat walls being curved can be thinner, and thus the cryostats less expensive.

The Muon System.

The parameters of the muon system are: 3 iron toroids magnetized to 2 T., weighing a total of 3400 tons, instrumented with three stations of proportional drift tubes (PDT's) arranged with one station between the calorimeter and iron, and 2 stations outside the iron. A prototype drift tube is shown schematically in figure 17. Test results on the non-bend coordinate using cosmic rays are shown in figure 18.⁸⁾

The design for muon detection is to have all wires parallel to the magnetic field lines and measure the coordinate in the bend plane with the more accurate precision of the drift time in the tube. The non-bend coordinate is obtained less accurately with a vernier pad current division system. Thus each of the 12,730 tubes has 5

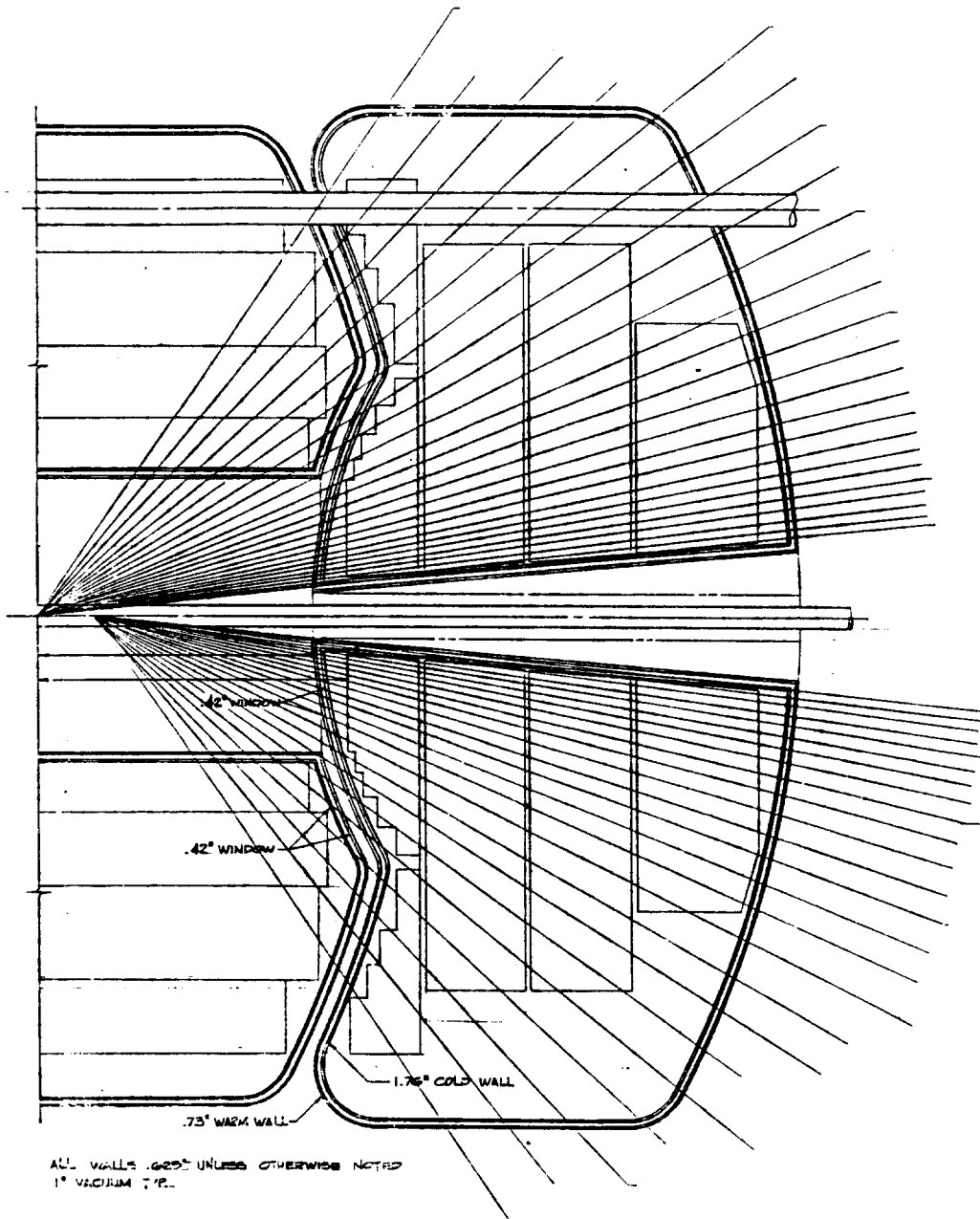


Figure 16

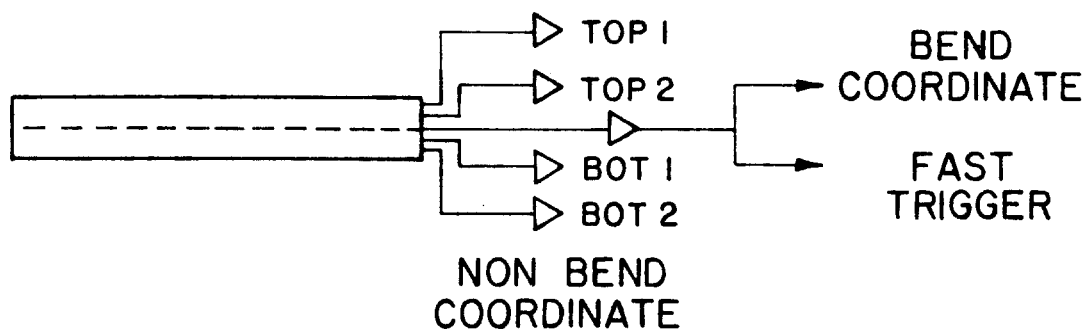
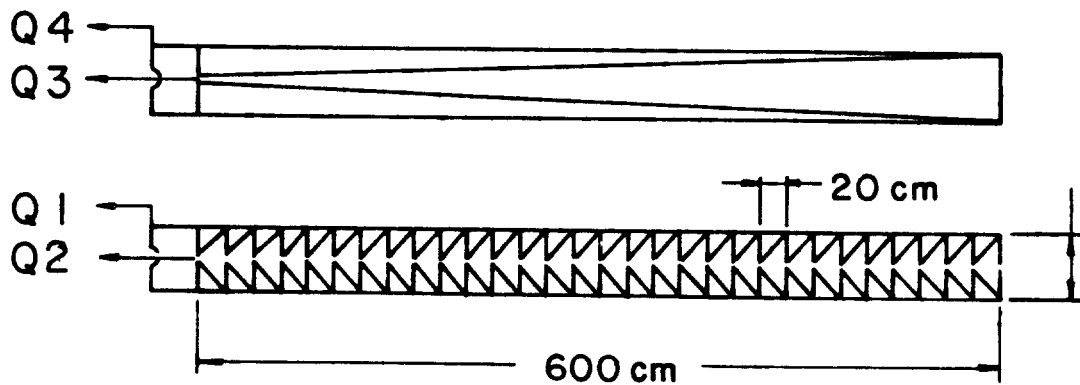
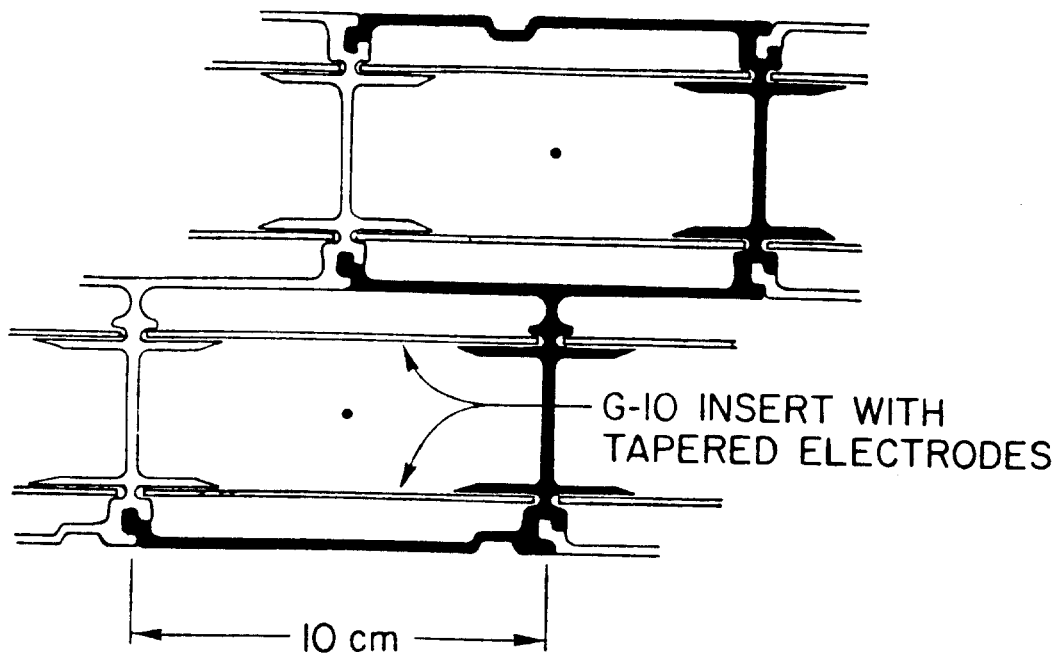


Figure 17

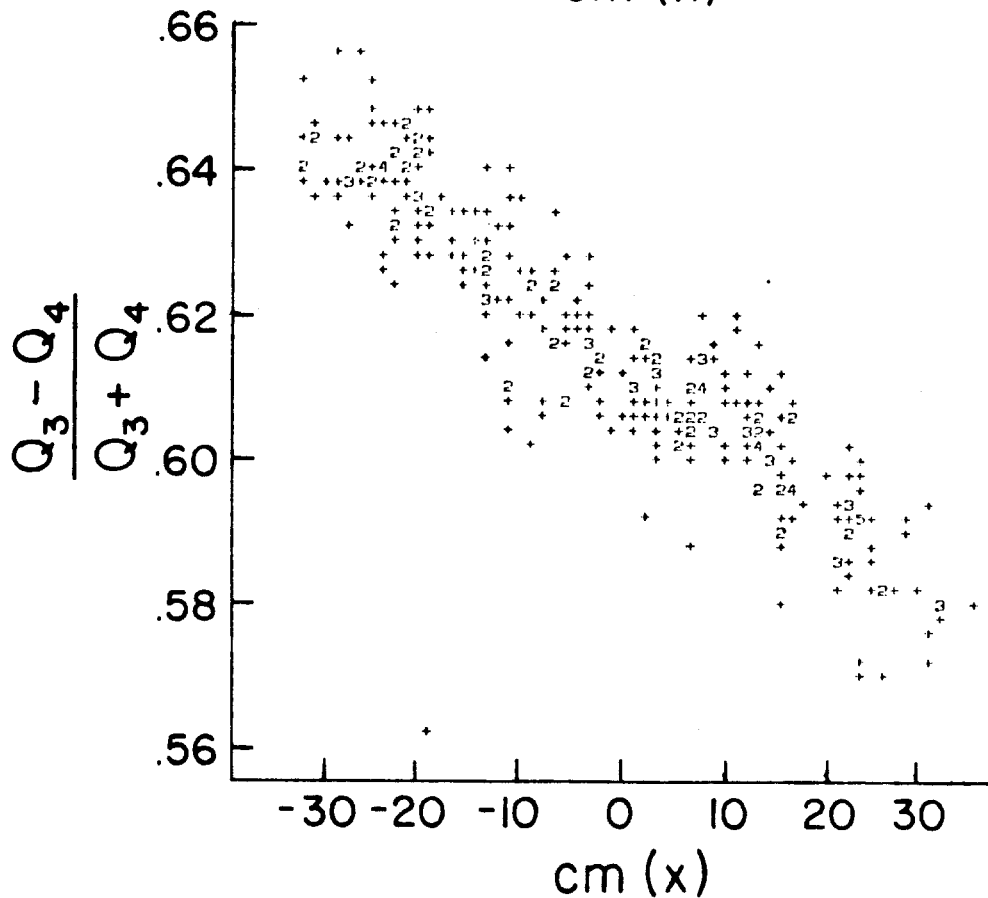
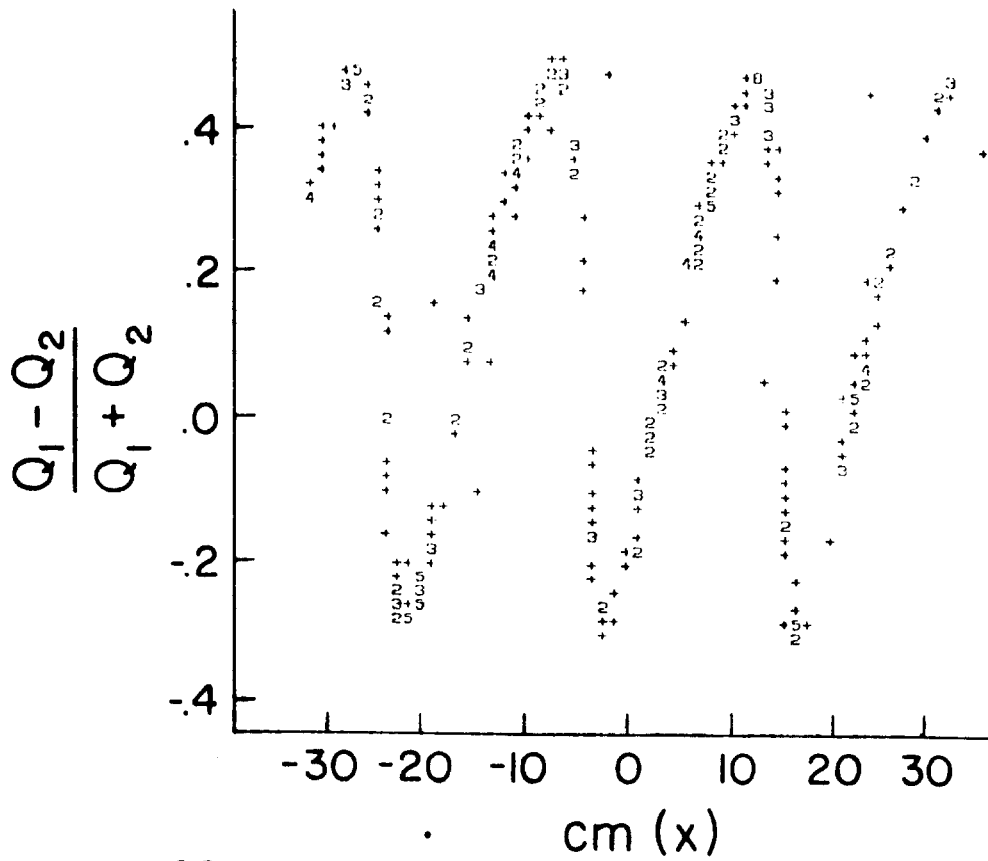


Figure 18

electronics outputs: a fast output from the wire for a trigger which also goes to the time digitizer, and four slow analog outputs. The time digitizers will have two hit capability since delta rays or other muon induced electromagnetic particles are fairly common. Overall system design goals are 500 microns resolution in the bend plane and 2 mm in the non-bend plane

Several different prototypes have been made and evaluated and more are being built. Much attention is going into the mechanical design in order to reduce the labor required and thus reduce the overall cost. We are also exploring faster gases which would then allow us to use wider, and fewer drift tubes, and still stay within the limit of time between bunch crossings.

Schedule.

A vigorous prototype and test program is being carried out on all systems in the D0 Detector. Various staging scenarios that would put part of the detector in place in 1987 are under discussion. However the fully built detector due mainly to rate of funding limitations could probably not be in place until 1989.

VII. ACKNOWLEDGEMENT

The warm hospitality of our host country, Italy, the occasion to visit the beautiful Aosta valley, the excellent organization of the conference by its organizers, and the opportunity to learn first hand from the accelerator, detector, and collider experience of our European colleagues, are all gratefully acknowledged.

References

1. Talks by M. Harrison, D. Theriot, and M. Marx at the Fourth Topical Workshop on Proton-Antiproton collider Physics. Berne. March 5 - 8, 1984.
2. Design Report, Tevatron 1 Project. FNAL. Sept. 1984. Design Report for the Fermilab Collider Detector Facility, Aug. 1981. Design Report, the D0 Experiment at the Fermilab \bar{p} -p Collider, November 1984.
3. S. Van der Meer, Stochastic Damping of Betatron Oscillations in the ISR, CERN/ISR-PO/72-31 (1972).
4. B. F. Bayanov et al., Nucl. Inst. Methods 190, 9(1981).
5. D. Bogert et al., "The Tevatron Control System, IEEE Trans. Nucl. Sci. NS-28, 2204 (1981).
6. A. Tollestrup. "CDF at Fermilab. A Progress Report." To be

published in the proceedings of the Aspen Winter Physics Conference. Jan. 6-12, 1985.

7. D. Green et al., "Hadron Shower and Muon Penetration in Thick Absorbers." 1985. To be published.
8. C. Brown et al., "E-740 Proportional Drift Tube Tests." Fermilab TM-1301, 2562.000. March, 1985.